

Retrieval of oceanic constituents from ocean color using simulated annealing

Pieter Kempeneers
Sindy Sterckx
Walter Debruyne
Vito, Boeretang 200,
B-2400 Mol, Belgium
Email: pieter.kempeneers@vito.be

Steve De Backer
Paul Scheunders
University of Antwerp
Groenenborgerlaan 171,
B-2020 Antwerpen, Belgium

Youngje Park
Kevin Ruddick
MUMM, Gulledele 100,
B-2100 Brussels, Belgium

Abstract—The color of the sea is determined by the contents of the water, especially the concentrations of suspended particulate matter (SPM), phytoplankton pigments such as chlorophyll (CHL) and colored dissolved organic matter (CDOM). Reversely, optical sensors that measure the water-leaving reflectance spectra allow us to calculate the desired concentration products. In this paper, a method is introduced that is valid for both case 1 and 2 waters. To this end, model is fitted to reflectance spectra, using simulated annealing for optimizing the mean square of the reflectance over all spectra.

I. INTRODUCTION

A variety of methods exists for the retrieval of water quality variables. A first is based on the decrease of the blue to green reflectance ratio as CHL is increased. It works well in oceanic waters, determined by phytoplankton and related degradation products. However, it fails in coastal and inland waters, where inorganic suspended matter and dissolved and particulate non-phytoplanktonic matter also affect optical properties. Another method calculates CHL using the red to near infrared ratio, which is effective for high concentrations, but is inaccurate for low concentrations. The multi-band inversion of a bio-optical model is a different kind of method that has found great interest. It calculates concentrations for SPM, CHL and CDOM simultaneously and it is based on a multi-band inversion of a bio-optical model. The forward model, such as the one introduced by Kirk [1] and Morel and Gentili [2] relates the reflectance just below the water surface to the absorption and back scattering coefficients. Inversion has already been proposed in the literature through neural networks [3] or matrix inversion [4]. The matrix inversion is restricted to linear forward models only, in which case an analytical expression can be found. However, these linear models have constraints. One of the typical problems of this approach is the presence of negative concentration values when applying to real data. Neural networks on the other hand have to be trained with large data sets. Collecting field data at sea is time consuming and therefore extremely expensive. As a result, existing databases are rather sparse. An alternative approach is to use simulated data for training, at the risk of poor generalization.

Here concentration values are estimated by fitting a model to

reflectance spectra. Some optimization schedule and criterion is needed. We have used a simulated annealing technique (SA), optimizing the mean square of the reflectance error over all spectra.

II. ANALYTICAL MODEL FOR THE IRRADIANCE REFLECTANCE

The subsurface reflectance can be related to the remote sensing reflectance measured from (far) above the water surface [5]. Through models, the reflectance is related to the backscattering and absorption coefficients, from which water quality variables can be derived. A complete derivation of the analytical model for the irradiance reflectance can be found in [6].

For simulations of subsurface reflectance, we consider, throughout this paper, water bodies which consists of four optically active components: pure seawater (w), phytoplankton (ϕ), non-algal particles (NAP) and CDOM. Also for comparison with matrix inversion results (see section IV), we use a linearized IOP model.

The total absorption coefficient (a) is a sum of contributions from the four components:

$$a(\lambda) = a_w(\lambda) + a_\phi(\lambda) + a_{\text{NAP}}(\lambda) + a_{\text{CDOM}}(\lambda) \quad (1)$$

The water absorption coefficient $a_w(\lambda)$ was taken from Pope and Fry [7]. Phytoplankton absorption coefficient $a_\phi(\lambda)$ is computed as:

$$a_\phi(\lambda) = \text{BricA} * \text{CHL}, \quad (2)$$

with BricA taken from [8]. The non-algal particle absorption a_{NAP} is assumed as:

$$a_{\text{NAP}}(\lambda) = a_{\text{NAP}}(443) \exp(-S_{\text{NAP}}(\lambda - 443)) \quad (3)$$

with $S_{\text{NAP}} = 0.0116 \text{ nm}^{-1}$ for the North Sea [9] and $a_{\text{NAP}}(443)$ assumed to be proportional to the suspended particulate matter concentration (SPM) with the constant of proportionality 0.033. Assuming that $\text{SPM}_{\text{NAP}} = 0.83 \text{ SPM}$ [9], equation (3) can be written as:

$$a_{\text{NAP}}(\lambda) = \frac{0.033}{0.83} \times \text{SPM}_{\text{NAP}} \times \exp(-0.0116(\lambda - 443)) \quad (4)$$

The CDOM absorption has a spectral dependence similar to $a_{\text{NAP}}(\lambda)$:

$$a_{\text{CDOM}}(\lambda) = a_{\text{CDOM}}(443) \exp(-S_{\text{CDOM}}(\lambda - 443)), \quad (5)$$

where $S_{\text{CDOM}} = 0.0167 \text{ nm}^{-1}$ for the North Sea [9].

Since the CDOM scattering is negligible, the total volume scattering function (VSF) can be written as:

$$\beta(\lambda, \theta) = \beta_w(\lambda, \theta) + \beta_\phi(\lambda, \theta) + \beta_{\text{NAP}}(\lambda, \theta), \quad (6)$$

where θ is the scattering angle. It is known that $\beta_\phi(\lambda, \theta)$ is highly variable depending on phytoplankton species and only weakly contributes to water reflectance (due to weak backscattering ratio). Therefore instead of using $\beta_\phi(\lambda, \theta)$ the scattering model of phytoplankton and covarying (associated) particles, $\beta_{\text{C}}(\lambda, \theta)$ was used. Defining SPM_{NC} to be a part of SPM which is not covarying with CHL, the VSF is decomposed as:

$$\beta(\lambda, \theta) = \beta_w(\lambda, \theta) + \beta_{\text{C}}(\lambda, \theta) + \beta_{\text{NC}}(\lambda, \theta), \quad (7)$$

This equation can be rewritten in terms of scattering coefficients $b(\lambda)$ and scattering phase functions $P(\theta)$:

$$b(\lambda)P(\theta) = b_w(\lambda)P_w(\theta) + b_{\text{C}}(\lambda)P_{\text{C}}(\theta) + b_{\text{NC}}(\lambda)P_{\text{NC}}(\theta) \quad (8)$$

For the simulation $b_w(\lambda)$ was taken from Smith and Baker [10]. The scattering coefficient due to phytoplankton and covarying particles $b_{\text{C}}(\lambda)$ is given as a function of CHL:

$$b_{\text{C}} = b_{\text{C}}(660) \times \left(\frac{660}{\lambda} \right)^{0.7}, \quad (9)$$

with $b_{\text{C}}(660) = 0.407 \times \text{CHL}$. The scattering phase function $P_{\text{C}}(\theta)$ is computed as a weighted combination of two Fournier-Forand phase functions so that the backscattering ratio should be

$$\frac{b_{b_{\text{C}}}}{b_{\text{C}}} = \tilde{b}_{b_{\text{C}}}(660) = 0.0096 \quad (10)$$

Details on how to make this scattering phase function can be found in [11].

The scattering coefficient due to non-covarying particles $b_{\text{NC}}(\lambda)$ is modeled as:

$$b_{\text{NC}}(\lambda) = b_{\text{NC}}(555) \left(\frac{555}{\lambda} \right)^n \quad (11)$$

It is assumed that b_{NC} is proportional to SPM_{NC} with $b_{\text{NC}}(\lambda)/\text{SPM}_{\text{NC}} = 0.54$ [12]. With SPM_{C} the dry weight of phytoplankton and covarying particles and $n = 0.4$, equation (11) can be rewritten as:

$$b_{\text{NC}}(\lambda) = 0.54 \times \text{SPM}_{\text{NC}} \times \left(\frac{555}{\lambda} \right)^{0.4} \quad (12)$$

The scattering phase function $P_{\text{NC}}(\theta)$ is computed in the same way as for $P_{\text{C}}(\theta)$ but using a constant backscattering ratio of 0.01833.

According to the IOP model described above, SPM_{NAP} is needed for absorption coefficients, while SPM_{NC} is required

for scattering coefficients. We assume the relationship between the quantities as follows:

$$\text{SPM} = \text{SPM}_{\text{C}} + \text{SPM}_{\text{NC}} = \text{SPM}_\phi + \text{SPM}_{\text{NAP}} \quad (13)$$

$$\text{SPM}_{\text{C}} = 0.234 \times \text{CHL} \quad (14)$$

$$\text{SPM}_\phi = 0.5 \times \text{SPM}_{\text{C}} \quad (15)$$

Notice that SPM_{C} is in g/m^3 and CHL is in mg/m^3 . With the equations above, the three unknown variables used for the simulations are CHL, SPM_{NC} and CDOM. We will further use the term SPM for SPM_{NC} .

III. METHODOLOGY

For this paper, the input irradiance reflectance (\mathbf{R}), is obtained through HYDROLIGHT simulations as explained in IV-A. For real imagery, this is the remote sensing reflectance measured from above the water surface. The optimizer will then try to fit a modeled reflectance $\hat{\mathbf{R}}$ to \mathbf{R} . The variables for the optimizer are the concentrations CDOM, CHL and SPM. We used the model from (16). Both f factors are implemented for comparison. The first depends on the backscattering ratio (with $b_b(w)$ the backscatter of water) [2] and thus on the concentrations CDOM, CHL and SPM. The latter depends only on the cosine of the sun zenith angle (μ_0) [13] and can therefore directly be used for the matrix inversion.

$$\begin{aligned} R(0-) &= f \frac{b_b}{a}, & (16) \\ f_{\text{Morel}} &= 0.63 + \left(-0.22 \frac{b_b(w)}{b_b} \right) - 0.05 \left(\frac{b_b(w)}{b_b} \right)^2 - \\ &\quad \left(0.31 - 0.25 \frac{b_b(w)}{b_b} \right) \mu_0 \\ f_{\text{Kirk}} &= (0.975 - 0.629 \mu_0) \end{aligned}$$

The f factor can be recalculated at each iteration, using the updated values needed for the model. Another way to deal with this factor is to treat it as an additional parameter to be estimated during the optimization. This option has some advantages as shown in IV.

The minimization criterion is defined in matrix notation as:

$$\text{minimization criterion} = (\mathbf{R} - \hat{\mathbf{R}}) \Sigma^{-1} (\mathbf{R} - \hat{\mathbf{R}})^t, \quad (17)$$

where \mathbf{R} and $\hat{\mathbf{R}}$ are vectors containing the measured and modeled reflectance spectra respectively for all wavelengths and Σ is the covariance matrix of the signal noise. A similar approach was followed in [14], but with a fixed noise value of the measured reflectance. We have adapted this formula for a band selective signal to noise ratio. When this is known for a specific sensor, this information can be used for weighting the criterion.

In general, the criterion in (17) will contain many local minima. The global minimum will thus not be obtained straight forward from an analytical result. In [14] the authors used a downhill simplex method. In this paper, we used simulated annealing [15], which is considered more reliable for finding global minima.

Simulated annealing was also applied in a similar context in [16]. However, the authors used the optimization process only once to obtain a unique set of parameters that optimize the semi-analytical model. In this paper, the optimization is used to retrieve the concentration values for each individual measured reflectance. A draw back of this method is that it is time consuming due to its iterative approach. As large processing capacity becomes widely available through low priced personal computers, this technique is no longer limited to small sized test samples, but can well be used for real imagery. The processing time depends on the spectral resolution (number of bands) of the signal. On a Pentium IV single 2GHz processor machine an image containing 48 bands was processed with 30 pixels per second.

Boundary constraints for the concentrations are easy to set, as well as putting initial values for the iterative search to the optimum. Constraining and intelligently guessing initial values can speed up the process. In case of image data, the concentrations of the previously found pixel can be used as initial value for the next, as nearby pixels will likely to have similar values.

Using hyperspectral data, the optimization process for fitting the reflectance spectra is constrained by a large number of bands.

The proposed methodology is not limited to a specific sensor. However, hyperspectral sensors with their larger number of bands will constrain the optimization process more, making it more robust. Fewer constraints may lead to ambiguous results.

IV. EXPERIMENTS

A. HYDROLIGHT simulations

Experimental results are obtained using a monte carlo simulation. Random concentrations for CDOM, CHL and SPM are used as input for HYDROLIGHT 4.2 [17], a state of the art underwater radiative transfer model. The obtained dataset consists of subsurface irradiance reflectance spectra $R(0-)$ from 400 to 800nm for a large range of chlorophyll (CHL), suspended particulate matter (SPM) and colored dissolved organic matter (CDOM) concentrations and geometry conditions (sun and view angles). A list of parameters for the HYDROLIGHT simulation is summarized in Table I. The concentrations are randomly varied between the boundaries listed.

TABLE I
HYDROLIGHT PARAMETERS

Parameter	Value
Solar zenith angle	0°, 15°, 30°, 60°
View zenith angle	0°, 30.38°, 60.13°
Relative azimuth angle	0°, 90°, 180°
Wind speed	5 m/s
Sky condition	clear (model of Harrison and Coombes)
CDOM	0-1 g/m ³
CHL	0-30 mg/m ³
SPM	0-100 l/m ³

Troughout the simulations optically deep water, which is believed true for turbid waters, and homogeneous water column was assumed. In the current dataset, inelastic scattering (such as chlorophyll fluorescence and Raman scattering) and bottom reflectance was not considered.

Published IOP models based on measurements in the North Sea were used as far as available. Since no published phytoplankton absorption model for turbid waters exists, an oceanic water model for phytoplankton absorption was adopted. Details on the IOP models used in the simulations were described earlier in section II.

B. Results and Discussion

The concentrations for CDOM, CHL and SPM are retrieved first through matrix inversion and compared to the simulating annealing technique (figures 1,2 and 3 respectively). The sun zenith angle is used for calculating the f value according to Kirk in (16). Obviously, the Kirk model (represented in the figures by square dots) is too simplified for the heterogeneity of angles and concentrations. Moreover, negative values are obtained, ranging from -51 to 49 mg/m³ for CHL concentrations. For SPM, the obtained values by inversion are good for low concentrations, but deteriorate from 20 g/m³ onwards. Finally, the model has most difficulties with concentrations of CDOM.

When optimization (SA) is applied, the f value can be calculated for each iteration, as explained above. For this study, it has been calculated using Morel and Gentili in equation (16). The concentrations obtained for CDOM, CHL and SPM are shown in the figures as plus signs. The results are much more robust for different sun zenith angles. The concentrations are also guaranteed to be positive, because of the constraints used.

Finally, figure 4 shows the modeled irradiance reflectance for different models for a case of high CHL and SPM. The reflectance spectrum as output of HYDROLIGHT is shown as a reference. Simulated annealing has been applied to these models to fit the modeled reflectance irradiance to the simulated reflectance. The concentrations are set during the optimization process. For one curve, the f value is also optimized instead of calculating via one of the equations in (16). It is shown that for this example the modeled reflectance is closer to the true (simulated) reflectance. Especially the retrieval for SPM will improve using this method. This is part of ongoing research, as well as the application of other non-linear models.

ACKNOWLEDGMENT

The authors would like to thank the Belgian Science Policy Office for funding this research.

REFERENCES

- [1] J. Kirk, *Light & Photosynthesis in Aquatic Ecosystems*. Cambridge: Cambridge University Press, 1994.
- [2] A. Morel and B. Gentili, "Diffuse reflectance of oceanic waters. ii. bidirectional aspects," *Applied Optics*, vol. 32, pp. 6864-6879, 1993.
- [3] H. Schiller and R. Doerffer, "Neural network for emulation of an inverse model - operational derivation of case ii water properties from meris data," *irs*, vol. 20(9), pp. 1735-1746, 1999.

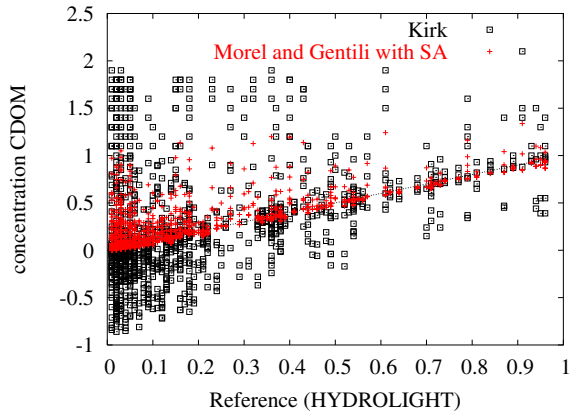


Fig. 1. Scatterplot for CDOM concentration comparing inverse matrix with Kirk to Simulated Annealing (SA) with Morel and Gentili

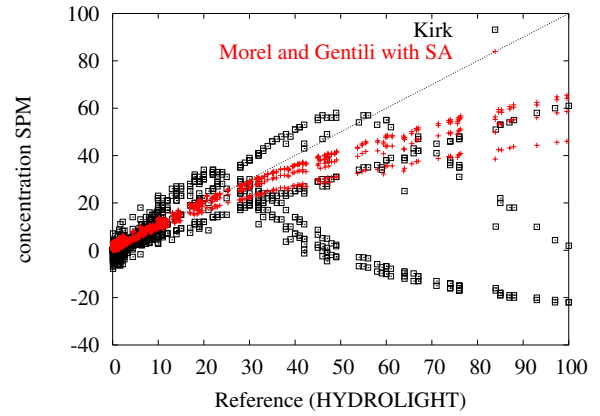


Fig. 3. Scatterplot for SPM concentration comparing inverse matrix with Kirk to Simulated Annealing (SA) with Morel and Gentili

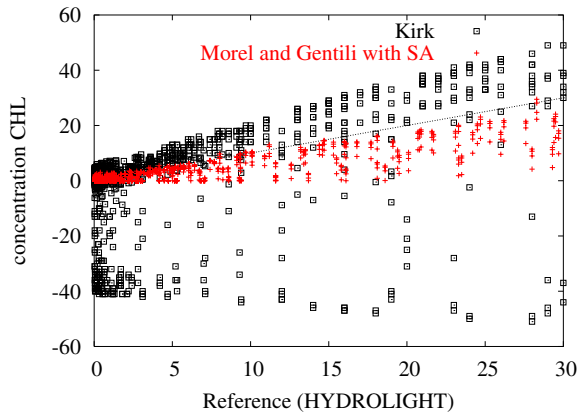


Fig. 2. Scatterplot for CHL concentration comparing inverse matrix with Kirk to Simulated Annealing (SA) with Morel and Gentili

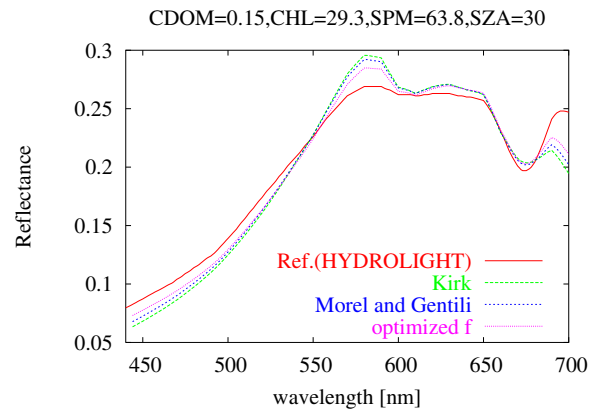


Fig. 4. Reflectance fit according to the different models. The model of Morel and Gentili outperforms the model of Kirk, while the best fit is obtained when the f factor is optimized through the same SA technique that optimized the concentrations.

[4] F.E.Hoge, C.W.Wright, P. Lyon, R. Swift, and J. Yungel, "Satellite retrieval of inherent optical properties by inversion of an oceanic radiance model: a preliminary algorithm," *Applied Optics*, vol. 38(3), pp. 495–504, 1999.

[5] F. D. van der Meer and S. M. de Jong, *Imaging Spectrometry, Basic Principles and Prospective Applications*. Dordrecht: Kluwer Academic Publishers, 2001.

[6] E. Aas, "Two-stream irradiance model for deep waters," *Applied Optics*, vol. 26, pp. 2095–2101, 1987.

[7] R. M. Pope and E. S. Fry, "Absorption spectrum (380–700nm) of pure water. ii. integrating cavity measurements," *Applied Optics*, vol. 36, pp. 8710–8723, 1997.

[8] A. M. A.Bricaud, M. Babin and H. Claustre, "Variability in the chlorophyll-specific absorption coefficients of natural phytoplankton: Analysis and parameterization," *Journal on Geophysical Research*, vol. 100, pp. 13 321–13 332, 1995.

[9] M. Babin, D. Stramski, G. Ferrari, H. Claustre, A. Bricaud, G. Obolensky, and N. Hoepffner, "Variations in the light absorption coefficients of phytoplankton, nonalgal particles, and dissolved organic matter in coastal waters around europe," *Journal on Geophysical Research*, vol. 108, p. 3211, 2003.

[10] R. C. Smith and K. Baker, "Optical properties of the clearest natural waters (200–800 nm)," *Applied Optics*, vol. 20(2), pp. 177–184, 1981.

[11] Y. Park and K. Ruddick, "Model of remote-sensing reflectance including bidirectional effects for case 1 and case 2 waters," *Applied Optics*, vol. 44, pp. 1236–1249, 2005.

[12] M. Babin, A. Morel, V. Fournier-Sicre, F. Fell, and D. Stramski, "Light

scattering properties of marine particles in coastal and open waters as related to the particle mass concentration," *Limnol. Oceanogr.*, vol. 48, pp. 843–859, 2003.

[13] J. Kirk, "Characteristics of the light field in highly turbid waters: a monte carlo study," *Limnol. Oceanogr.*, vol. 39, pp. 702–706, 1994.

[14] K. H. L. S. C. Liew, A. S. Chia and L. K. Kwoh, "Modeling the reflectance spectra of tropical coastal waters," *SPIE Proceedings on Optical Science and Technology*, vol. 4488, pp. 248–255, 2001.

[15] S. Kirkpatrick, C. D. Gelatt, and M. P. Vecchi, "Optimization by simulated annealing," *Science, Number 4598, 13 May 1983*, vol. 220, 4598, pp. 671–680, 1983.

[16] D. S. S. Maritorea and A. Peterson, "Optimization of a semi-analytical ocean color model for global scale applications," *Applied Optics*, vol. 41 (15), pp. 2705–2714, 2002.

[17] L. C. D. Mobley, *Hydrolight 4.2 Technical Documentation*. Redmond Washington: Sequoia Scientific, Inc., 2002.